

Dynamic Observation Study of the Crystallization Process in Sb-based Phase Change Materials

Naoki Shimidzu^{*1,2}, Toshikazu Nagatsuka², Yusuke Magara³, Norihiko Ishii¹, Nobuhiro Kinoshita¹, and Katsuaki Sato²

¹ Science and Technical Research Laboratories NHK, 1-10-11, Kinuta, Setagaya-ku, Tokyo, 157-8510, Japan

² Tokyo University of Agriculture and Technology, 2-24-16, Nakacho, Koganei, Tokyo 184-8588, Japan

³ Tokyo Denki University, 2-2 Kanda-Nishiki-cho, Chiyoda-ku, Tokyo 101-8457, Japan

A streak-camera system for observation of high-speed crystallization processes induced by a laser irradiation in phase-change (PC) recording materials has been developed. A distinct difference in the time-sequential development of the crystallized region was observed in two different types of PC materials; i.e., $\text{Sb}_{78}\text{Te}_{22}$ (eutectic composition) and $\text{Ge}_2\text{Sb}_2\text{Te}_5$ (pseudo-binary alloy) films. Taking into account a thermal simulation analyses, the observed difference has been interpreted in terms of the different crystallization process. It is concluded that $\text{Sb}_{78}\text{Te}_{22}$, which is the growth-dominant type, is suited for high-speed high-density recording.

KEYWORDS : phase change materials, optical recording, dynamic observation, streak camera

Phase-change (PC) recording materials are attracting an attention as materials for rewritable high-speed optical disks¹⁾ and phase-change RAM (PC RAM),²⁾ that use difference in the reflectivity or the electrical resistivity between crystalline and amorphous phases. These materials undergo a phase change in less than a few tens of nanoseconds. Substantial reduction of the time for the phase change from amorphous to crystalline states is strongly required since recording speed is governed by an erasing (amorphous-to-crystalline change) speed prior to the recording (crystalline-to-amorphous change).

Observation of the crystallization process in PC materials has been performed by pursuing a reflectivity change or tracing a thermal analysis curve during the amorphous-to-crystalline transition, as well as by using an X-ray structural analysis.^{3, 4)} However, details of the phase-change process have not been elucidated yet. Although Kolobov et al. have clarified from detailed XAFS and XANES analysis that the phase-change process is not a real phase transition from amorphous to crystalline states, but rather a change between two crystalline phases, they do not refer to the lack of long range order in the X-ray diffraction (XRD) patterns in the so-called “amorphous state”.⁶⁾ Therefore, there is still much more investigations to be done in order to understand the phase-change mechanism, in particular dynamic observation of the phase-change process.

To observe a high-speed phase transformation from “amorphous” to “crystalline” state induced by laser irradiation in the PC materials, we have constructed a novel dynamic observation system employing a streak-camera. As specimens for the present study we adopted $\text{Ge}_2\text{Sb}_2\text{Te}_5$ and $\text{Sb}_{78}\text{Te}_{22}$

films, the former being a typical example of nucleation-dominant materials while the latter growth-dominant materials. In $\text{Ge}_2\text{Sb}_2\text{Te}_5$, nucleation starts randomly and uniformly over the laser-irradiated spot, whereas in $\text{Sb}_{78}\text{Te}_{22}$ crystallization proceeds primarily from the amorphous-crystalline boundaries prior to the growth.

The PC samples used in this study have been fabricated on a glass substrate by rf-magnetron sputtering from the corresponding targets in an Ar gas atmosphere using an rf-power of $1.3\text{W}/\text{cm}^2$. Sputtering conditions such as rf power and Ar gas pressure were controlled in order to form amorphous films. Most of the measurements were performed on as-sputtered amorphous films. For comparison, previously annealed samples were also examined.

We determined the crystallization temperature T_x in these films from an exothermal peak temperature in a differential scanning calorimetry (DSC). In the $\text{Sb}_{78}\text{Te}_{22}$ film, only one exothermal peak was observed at 153°C , whereas in $\text{Ge}_2\text{Sb}_2\text{Te}_5$ two peaks appeared at 185°C and at 274°C , the former being a transition from amorphous to metastable fcc phase and the latter a transition from metastable fcc to stable hcp phase. In X-ray diffraction studies as-sputtered films show no diffraction peaks, while films annealed above 200°C showed prominent diffraction peaks.

For the dynamic observation of the $\text{Ge}_2\text{Sb}_2\text{Te}_5$ film, a film stack with dielectric ZnS layers was used in order to prevent damages caused by sublimation of the film and also to enhance optical contrast between crystalline and amorphous states. The refractive index n and extinction coefficient k of the $\text{Ge}_2\text{Sb}_2\text{Te}_5$ film and ZnS film were obtained using an ellipsometry measurement, and the optimum film thickness was calculated using the OPTAS FILM analysis software. The layer structure of the sample is shown in Fig. 1.

Experimental setup of the system for a dynamic observation is illustrated in Fig. 2. The system consists of a laser diode (LD) (wavelength: 405 nm), an objective lens (60X, numerical aperture: 0.7), a Xe flash lamp (1 J/pulse, Hamamatsu Photonics L7684), a streak camera (Hamamatsu Photonics C7700 with a built-in image intensifier V7669U-06) and a cooled CCD camera (1344 x 1024 pixels, Hamamatsu Photonics C4742-95-12ER). The light from the LD is focused on the substrate side of the film by using an objective lens to irradiate the sample to cause a phase-change. The streak camera observation was carried out from the opposite side of the film illuminated by using the Xe flash lamp. The streak camera is capable of a rapid sweep of an image and is suited for high-speed dynamic observation because of its high sensitivity by the use of an image-intensifier. After irradiation the LD is switched off during the streak-camera observation. A sharp-cut low-pass filter was employed to prevent an afterglow of the LD enter the streak camera.

In order to observe the fast phase-change process, the operation timing of the LD light source, flash lamp, streak camera, and the like are accurately controlled by a gate-pulse controller. The sweep timing of the streak-camera is synchronized to the start of the Xe flash lamp illumination, while the start timing of the Xe flash lamp is changed stepwise with $1\ \mu\text{s}$ interval from the gate pulse, to expand the observation time, since the intensity of the flash lamp is only constant for $1\ \mu\text{s}$. The power of the LD is 3.1 mW. The laser spot size on the film surface is $1.5\ \mu\text{m}$ in diameter. The observation is performed as the temporal change of the spatial image on the sample film, with a laser irradiation time of $10\ \mu\text{s}$ and a streak-camera sweep time of $1\ \mu\text{s}$.

The results of dynamic observation of the crystallization processes of $\text{Sb}_{78}\text{Te}_{22}$ and $\text{Ge}_2\text{Sb}_2\text{Te}_5$ film are shown in Figs. 3(a) and 3(b), respectively.⁵⁾ The vertical axis shows the elapsed time after the start of an LD irradiation, and the horizontal axis shows the position in one-dimensional image of the film surface. The bright area around the center of the image is considered to be a crystallized portion. We believe this result is the first direct dynamic observation of crystal growth process subsequent to laser irradiation in phase-change materials.

In the $\text{Sb}_{78}\text{Te}_{22}$ film (Fig. 3(a)), crystallization begins at 1.2 μs after the start of laser irradiation, while in the $\text{Ge}_2\text{Sb}_2\text{Te}_5$ film it becomes observable from 5.3 μs after the start. In addition, in the $\text{Sb}_{78}\text{Te}_{22}$ film, a lateral expansion of the crystallized portion is clearly observed. The growth of the crystallized area finally ends with the spot size of 2.7 μm in diameter which is wider than the beam diameter. The speed of crystal growth evaluated from the experiment is 0.28 m/s. On the other hand, in the $\text{Ge}_2\text{Sb}_2\text{Te}_5$ films (Fig. 3(b)) no distinct change is observed in the diameter of the crystallized portion while an increase in the intensity of the crystallized area is observed as seen in the cross-sectional profile of Fig. 3(b).

Thermal analysis has been carried out, in which the temporal change of the temperature in the region irradiated by the laser has been analyzed using a LASMA-P software (Fuji Research Inst. Corp.). The condition for calculating temperature distribution caused by the laser irradiation is shown in Table 1. The calculated results of the temporal change in the temperature profile of $\text{Sb}_{78}\text{Te}_{22}$ and $\text{Ge}_2\text{Sb}_2\text{Te}_5$ are shown in the right-hand side of the streak-camera signal in Figs. 3(a) and 3(b), respectively. It is found that temperature contours corresponding to T_x ($\approx 200^\circ\text{C}$) are almost the same for both materials. Therefore we can safely assume that the difference in the observed streak-camera image is not a consequence of different thermal properties but of the different crystallization phenomena.

Taking into account the results of the thermal analysis, the experimental dynamic observation can be explained as follows: In the eutectic $\text{Sb}_{78}\text{Te}_{22}$ film a crystal nucleus appear in the center of the laser spot, followed by the growth-dominant crystallization as schematically illustrated in Fig. 4(a), in which crystallization starts at the interface between the crystalline area and the amorphous surrounding. On the other hand in the pseudo-alloy $\text{Ge}_2\text{Sb}_2\text{Te}_5$ a nucleation-dominant crystallization process occurs, nucleation taking place in the whole area of the laser irradiated amorphous area, followed by a growth of the crystallites from the nuclei until they coalesce as shown in Fig. 4(b).

Crystallization in the $\text{Ge}_2\text{Sb}_2\text{Te}_5$ film becomes only observable at a time span of 5 μs after LD irradiation as shown in Fig. 3(b), despite the formation time of the crystal nucleus is known to be as short as 50 to 100 ns.⁷⁾ We consider that even though a lot of crystallites appear in the irradiated area they are too small to be observed due to the resolution limit of our system, and become observable only after they grow sufficiently large in size.

Complete crystallization time of a nucleation-dominant $\text{Ge}_2\text{Sb}_2\text{Te}_5$ film seems to be insensitive to the size of amorphous mark. On the other hand, a growth-dominant $\text{Sb}_{78}\text{Te}_{22}$ film strongly it depends on the size. The smaller becomes the mark size, the shorter is the crystallization time. We conclude that $\text{Sb}_{78}\text{Te}_{22}$ film is more adequate than $\text{Ge}_2\text{Sb}_2\text{Te}_5$ film for high-speed high-density recording materials.

Acknowledgements This research has been conducted as a part of the 21st Century COE Program of "Future Nano Materials" in Tokyo University of Agriculture and Technology.

References

- [1] N.Ishii, N.Kinoshita, M.Kishida, N.Shimidzu, H.Tokumaru, Y.Fujita, and J.Numazawa: Tech. Digest of EPCOS2003 (2003) 15.
- [2] S. Lai and T. Lowrey: Tech. Digest of IEDM, **36** (2001) 1.
- [3] N. Yamada, E. Ohno, K. Nishiuchi, and N. Akahira: J. Appl. Phys. **69** (1991) 2849.
- [4] T. Matsunaga and N. Yamada : Jpn. J. Appl. Phys, **41** (2002) 1674.
- [5] A.V. Kolobov, P. Fons, A.I. Frenkel, A. Ankudinov, J. Tominaga and T. Uruga: Nature Materials. **3** (2004)703.
- [6] N. Shimidzu, T. Nagatsuka, N .Ishii, N .Kinoshita and K. Sato: Phys. Status Solids (c) **3** (2006) 2858.
- [7] G.F. Zhou, H.J. Borg, J.C.N. Rijpers, M.H.R. Lankhorst and J.J.L. Horikx: Proc. SPIE **4090** (2000) 108.

Figure 1 : Layer structure

Figure 2: Experimental Setup

Figure 3: Dynamic observation results and thermal simulation

Figure 4: Schematic drawing of the crystallization process of two types of phase change materials

Table 1: Simulation parameters for thermal analysis

Figure 1 Layer structure

ZnS 30nm
SbTe or GeSbTe 40nm
ZnS 60nm
SiO ₂ Substrate

Figure 2 Experimental Setup

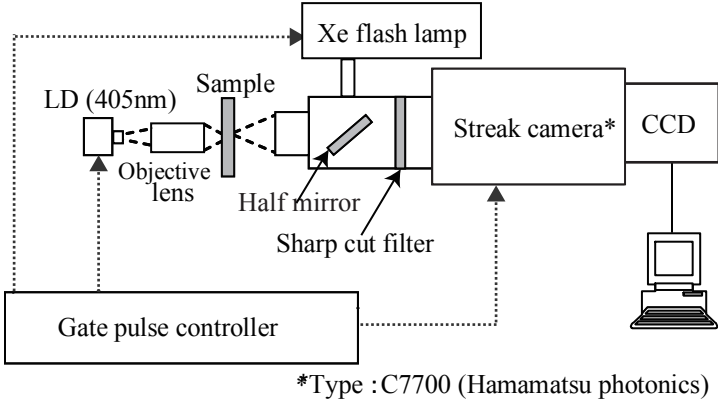


Figure 3 Dynamic observation results and thermal simulation

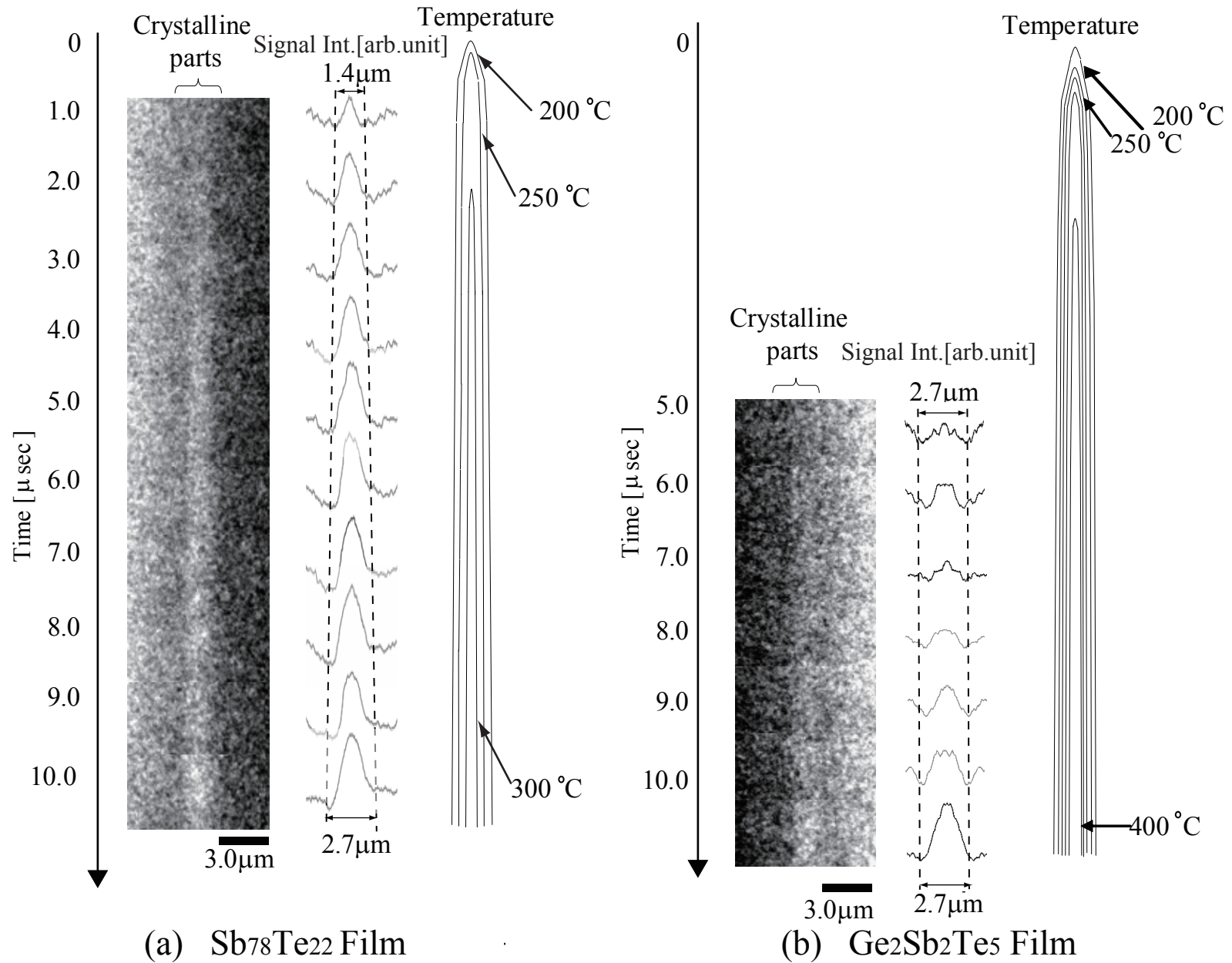


Figure 4 Schematic drawing of the crystallization process of two types of phase change materials

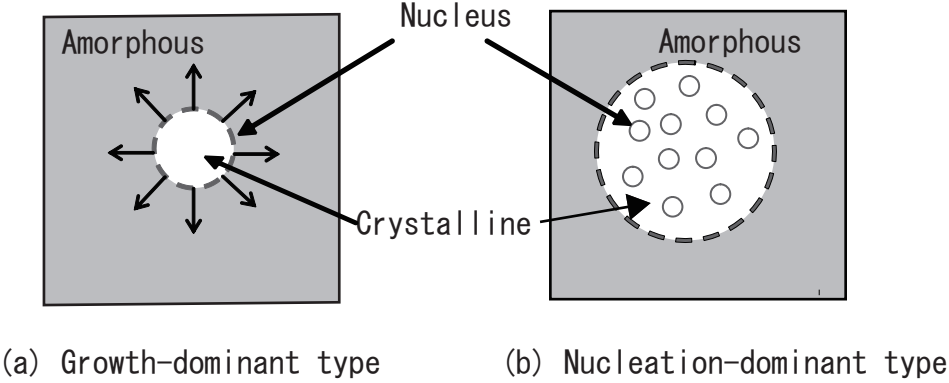


Table I. Simulation parameters for thermal analysis.

Specific heat (erg/(K•g))	Ge ₂ Sb ₂ Te ₅ Sb ₇ Te ₃ ZnS SiO ₂	2.09 x 10 ⁶ 2.08 x 10 ⁶ 5.62 x 10 ⁶ 1.26 x 10 ⁷
Thermal conductivity (erg/(cm•K•s))	Ge ₂ Sb ₂ Te ₅ Sb ₇ Te ₃ ZnS SiO ₂	3.78 x 10 ⁵ 1.77 x 10 ⁶ 4.27 x 10 ⁵ 2.23 x 10 ⁴
Density (g/cm ³)	Ge ₂ Sb ₂ Te ₅ Sb ₇ Te ₃ ZnS SiO ₂	6.15 6.56 3.65 1.20